

Selective infection of CD4⁺ effector memory T lymphocytes leads to preferential depletion of memory T lymphocytes in R5 HIV-1-infected humanized NOD/SCID/IL-2R γ ^{null} mice

Chuanyi Nie^{a,1}, Kei Sato^{a,1}, Naoko Misawa^a, Hiroko Kitayama^a, Hisanori Fujino^b, Hidefumi Hiramatsu^b, Toshio Heike^b, Tatsutoshi Nakahata^b, Yuetsu Tanaka^c, Mamoru Ito^d, Yoshio Koyanagi^{a,*}

^a Laboratory of Viral Pathogenesis, Institute for Virus Research, Kyoto University, 53 Shogoinkawara-cho, Sakyo-ku, Kyoto, Kyoto 606-8507, Japan

^b Department of Pediatrics, Graduate School of Medicine, Kyoto University, Kyoto, Kyoto 606-8501, Japan

^c Department of Immunology, Graduate School of Medicine, University of the Ryukyus, Nishihara, Okinawa 903-0125, Japan

^d Central Institute for Experimental Animals, Kawasaki, Kanagawa 216-0001, Japan

ARTICLE INFO

Article history:

Received 8 April 2009

Returned to author for revision 19 July 2009

Accepted 4 August 2009

Available online 9 September 2009

Keywords:

HIV-1 pathogenesis

Humanized mouse

Memory cell depletion

Productive infection

T cell activation

ABSTRACT

To investigate the events leading to the depletion of CD4⁺ T lymphocytes during long-term infection of human immunodeficiency virus type 1 (HIV-1), we infected human CD34⁺ cells-transplanted NOD/SCID/IL-2R γ ^{null} mice with CXCR4-tropic and CCR5-tropic HIV-1. CXCR4-tropic HIV-1-infected mice were quickly depleted of CD4⁺ thymocytes and both CD45RA⁺ naïve and CD45RA⁻ memory CD4⁺ T lymphocytes, while CCR5-tropic HIV-1-infected mice were preferentially depleted of CD45RA⁻ memory CD4⁺ T lymphocytes. Staining of HIV-1 p24 antigen revealed that CCR5-tropic HIV-1 preferentially infected effector memory T lymphocytes (T_{EM}) rather than central memory T lymphocytes. In addition, the majority of p24⁺ cells in CCR5-tropic HIV-1-infected mice were activated and in cycling phase. Taken together, our findings indicate that productive infection mainly takes place in the activated T_{EM} in cycling phase and further suggest that the predominant infection in T_{EM} would lead to the depletion of memory CD4⁺ T lymphocytes in CCR5-tropic HIV-1-infected mice.

© 2009 Elsevier Inc. All rights reserved.

Introduction

While it is evident that human immunodeficiency virus type 1 (HIV-1) causes acquired immunodeficiency syndrome (AIDS) in humans, the mechanism by which HIV-1 accomplishes this remains unclear. The gradual loss of peripheral blood (PB) CD4⁺ T lymphocytes during the asymptomatic phase of HIV-1 infection is one of the best prognostic predictors for the onset of AIDS (O'Brien et al., 1996), and CD4⁺ T lymphocyte depletion is thought to be a serious pathological change in AIDS (McCune, 2001).

To define the mechanisms behind CD4⁺ T lymphocyte depletion, a large number of studies have been conducted in humans, primates, and humanized mice by using HIV-1, simian immunodeficiency virus (SIV), and SIV/HIV-1 chimeric virus (SHIV) (Centlivre et al., 2007; Koyanagi et al., 2008; McCune, 2001). One of the important findings from previous studies was the dependence of pathogenesis on the co-receptor preference, CXCR4, and/or CCR5 (Berkowitz et al., 1998; Moore et al., 2004). CXCR4-tropic (X4) SHIV caused rapid and complete depletion of all subsets of CD4⁺ T lymphocytes in rhesus macaques, which led to death from immunodeficiency (Nishimura et

al., 2004). On the other hand, CCR5-tropic (R5) HIV-1 is the dominant type of HIV-1 found in patients, and clinical manifestation of HIV-1 infection resembles CCR5-tropic SIV infection (Berger, Murphy, and Farber, 1999). In both HIV-1-infected patients and SIV-infected rhesus macaques, the drastic onset of immunodeficiency is rare (Ambrose et al., 2007; McCune, 2001), and CD4⁺ T lymphocytes in PB slowly decrease in number, eventually leading to immunodeficiency.

X4 virus uses CXCR4 as the co-receptor and R5 virus uses CCR5 as the co-receptor for viral infection into target cells (Berger, Murphy, and Farber, 1999; Lusso, 2006). CXCR4 is expressed on naïve T lymphocytes and thymocytes, thus X4 HIV-1 can infect naïve T lymphocytes and thymocytes (Pedroza-Martins et al., 1998). It is well known that faster depletion of immature thymocytes and T lymphocytes is observed after the appearance of X4 HIV-1 (Berkowitz et al., 1998; Pedroza-Martins et al., 1998; Schnittman et al., 1990). On the contrary, CCR5 is primarily expressed on CD4⁺ effector memory T lymphocytes (T_{EM}) and macrophages but not on naïve and central memory CD4⁺ T lymphocytes (T_{CM}) (Sallusto, Geginat, and Lanzavecchia, 2004). Therefore, the selective infection of T_{EM} is thought to leave naïve T lymphocytes and T_{CM} intact. Depletion of T_{EM} by R5 virus has been studied in SIV-infected rhesus macaques (Brenchley et al., 2004; Li et al., 2005). In 14–28 days following infection, the population of extra-lymphoid CCR5⁺ T_{EM} was depleted up to 90% (Centlivre et al., 2007; Mattapallil et al., 2005; Okoye et al., 2007). At

* Corresponding author. Fax: +81 75 751 4812.

E-mail address: ykoyanag@virus.kyoto-u.ac.jp (Y. Koyanagi).

¹ These authors contributed equally to this study.

the same time, an obvious reduction in CD4⁺ T lymphocytes was not found in the PB. In an attempt to compensate for the loss of CCR5⁺ T_{EM}, CCR5⁻ T_{CM} was persistently activated and divided in order to prevent the collapse of the T_{EM} compartment (Brenchley, Price, and Douek, 2006). However, CCR5⁻ T_{CM} lose their regenerative capability after prolonged period of proliferation, leading to decrease in both T_{CM} and T_{EM} compartments (Brenchley, Price, and Douek, 2006). This continuous shortage in CCR5⁺ T_{EM} and accompanying CCR5⁻ T_{CM} exhaustion are thought to play an important role in the progression to AIDS (Centlivre et al., 2007). Although the overloading of CD4⁺ memory T lymphocyte homeostasis serves a compelling model of immunodeficiency in SIV infection, its relevance in HIV-1 infection is still poorly defined. Therefore, it is necessary that memory T lymphocyte infection is studied in an experimental animal model reconstituted with competent human immune cells.

To investigate the dynamics of CD4⁺ T lymphocyte depletion following HIV-1 infection and the status of HIV-1-producing cells *in vivo*, we infected human CD34⁺ cells-transplanted newborn NOG mice (NOG-hCD34 mice) with HIV-1_{JR-CSF} (R5 HIV-1) or HIV-1_{NL4-3}

(X4 HIV-1). Our findings indicate that X4 HIV-1 infection can cause the depletion of CD4⁺ thymocytes which results in the reduction in both naïve and memory T lymphocytes, while R5 HIV-1 infection can selectively deplete memory CD4⁺ T lymphocytes. Further analyses indicate that R5 HIV-1 preferentially infects CCR7⁻ T_{EM} and that the infected cells are predominantly activated and in an actively proliferating state. These results suggest that preferential infection in the activated T_{EM} leads to selective depletion of memory CD4⁺ T lymphocytes in R5 HIV-1-infected patients.

Results

Kinetics of PB CD4⁺ T lymphocyte depletion in R5 and X4 HIV-1-infected mice

NOG-hCD34 mice were generated by human CD34⁺ hematopoietic stem cell transplantation into neonatal NOG mice as described previously (Baenziger et al., 2006; Traggiai et al., 2004). A significant level of human leukocytes was maintained in the whole PB of 13–44

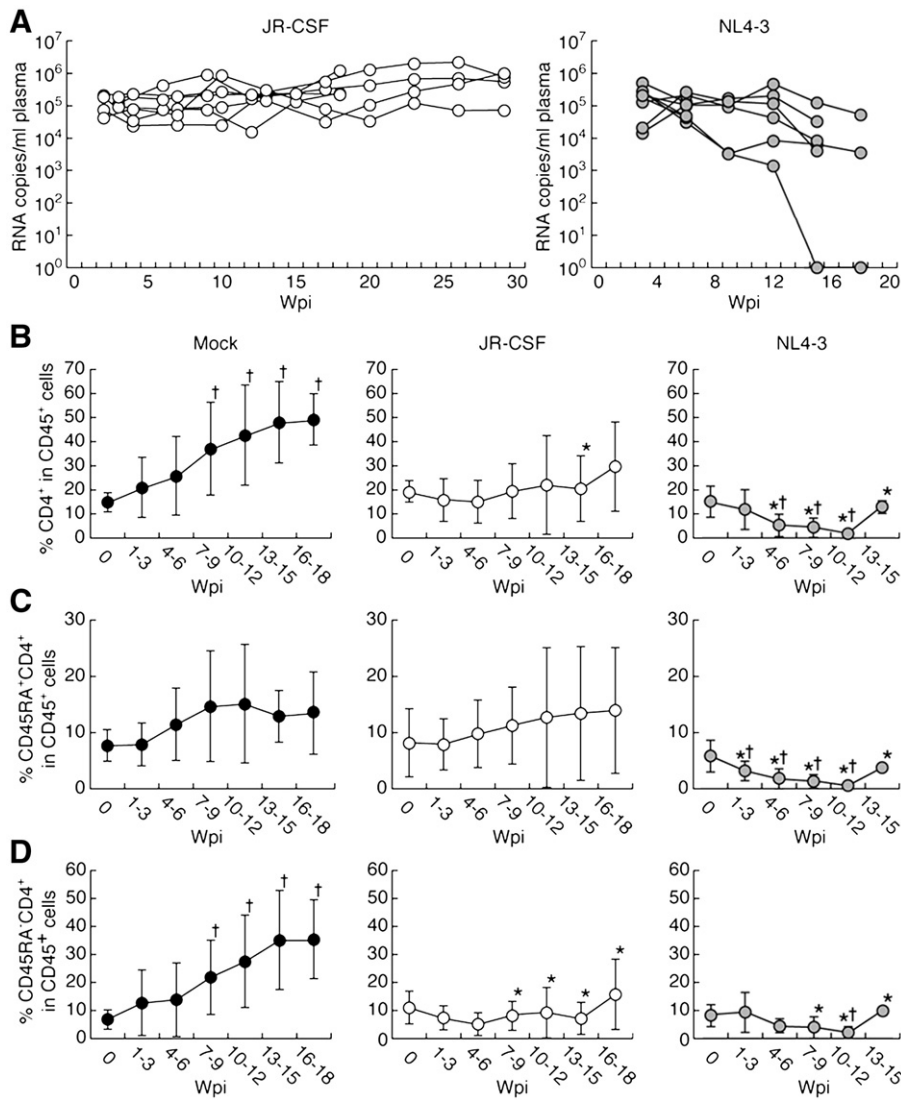


Fig. 1. Longitudinal analysis on plasma viral load and CD4⁺ T lymphocytes in the PB of R5 and X4 HIV-1-infected mice. NOG-hCD34 mice were intraperitoneally injected with 1 × 10⁵ TCID₅₀ of HIV-1_{JR-CSF} (n = 7) or HIV-1_{NL4-3} (n = 8) between 12 and 13 weeks olds. (A) The longitudinal analysis on the plasma viral load of HIV-1_{JR-CSF}-infected (left) and HIV-1_{NL4-3}-infected (right) mice. (B–D) PB was routinely sampled and analyzed for CD45RA expression in CD4⁺ T lymphocytes from mock-infected (n = 8), HIV-1_{JR-CSF}-infected (n = 7), and HIV-1_{NL4-3}-infected (n = 8) mice. We assigned data into 7 periodic groups (data taken at 0, between 1–3, 4–6, 7–9, 10–12, 13–15, and 16–18 wpi), and the average percentage and standard deviation were calculated using data obtained from each mouse during each time period. The percentages of CD4⁺ (B), CD45RA⁺CD4⁺ (C), and CD45RA⁻CD4⁺ (D) T lymphocytes in the peripheral CD45⁺ cells are shown. Error bars show standard deviations. Daggers represent statistical difference (P < 0.05) when compared to the value at 0 wpi, and asterisks represent statistical difference when compared to the value obtained from the mock-infected mice.

week old mice (Supplemental Fig. 1A). Hematopoietic and lymphoid organs such as thymus, bone marrow, spleen and lymph nodes were highly repopulated with human mononuclear cells (Supplemental Figs. 1B–E). The expression of CCR5 was mainly restricted within the CD45RA[−] memory subset in CD4⁺ T lymphocytes, and CXCR4 was broadly expressed on both naïve and memory T lymphocytes (Fig. 4C and data not shown) as observed in humans (Ebert and McColl, 2001).

NOG-hCD34 mice were inoculated with either an R5 HIV-1 (HIV-1_{JR-CSF}) or an X4 HIV-1 (HIV-1_{NL4-3}) between 12 and 13 weeks old. HIV-1 RNA was detected in the plasma of these mice as early as 3 weeks post-infection (wpi) and was maintained at high levels (1×10^4 to 10^6 copies per milliliter) until 28 wpi or until sacrificed (Fig. 1A). PB of these mice was then analyzed for longitudinal changes in CD4⁺ T lymphocytes by flow cytometry. In the PB of both HIV-1_{JR-CSF}-infected and HIV-1_{NL4-3}-infected mice, depletion of human CD4⁺ T lymphocytes was consistently found (Fig. 1B). In HIV-1_{NL4-3}-infected mice, both CD4⁺CD45RA⁺ naïve and CD4⁺CD45RA[−] memory T lymphocytes were depleted, whereas in HIV-1_{JR-CSF}-infected mice, CD4⁺CD45RA[−] memory T lymphocytes were specifically depleted (Figs. 1C and D). These data indicate that the infection with HIV-1_{NL4-3} caused faster and more severe depletion of both naïve and memory subsets of CD4⁺ T lymphocytes and the infection with HIV-1_{JR-CSF} preferentially depleted memory CD4⁺ T lymphocytes.

Thymopathy in X4 HIV-1-infected mice

To investigate the effect of HIV-1 infection on the thymopoiesis in NOG-hCD34 mice, the thymocytes from HIV-1-infected and mock-infected mice were isolated and were analyzed with flow cytometry. In mock-infected and HIV-1_{JR-CSF}-infected mice, CD4 and CD8 double positive (DP) thymocytes were predominant (Fig. 2A). CD4 single positive (SP) and CD8 SP thymocytes together made up a major fraction of the thymocyte population, and double negative (DN) thymocytes were only a minor fraction. In contrast, thymi from HIV-1_{NL4-3}-infected mice were severely depleted of both CD4 SP thymocytes and DP thymocytes (Figs. 2A–C). Furthermore, thymi from HIV-1_{NL4-3}-infected mice had greatly reduced number of all subsets of thymocytes (Fig. 2D). CD4 SP and DP thymocytes showed the greatest (approximately 100-fold) reduction, while CD8 SP thymocytes showed relatively milder (approximately 10-fold) reduction (Fig. 2D). These data indicate that infection with HIV-1_{NL4-3} led to

disturbed thymopoiesis and that HIV-1_{JR-CSF} infection did not affect thymopoiesis.

Histological detection of p24-positive cells

HIV-1 p24-positive cells productively produce HIV-1 virions. Since human CD45⁺ mononuclear cells were very few or absent in HIV-1_{NL4-3}-infected mice when sacrificed, they were not further analyzed (data not shown). As presented in Fig. 3, the immunohistological staining showed the presence of HIV-1 p24-positive cells in all of the bone marrow, spleen, and lymph nodes. HIV-1 p24 staining colocalized with CD4 staining. Also, a larger percentage of cells seemed to be productively infected with HIV-1 in the spleen and lymph nodes.

Depletion of splenic memory CD4⁺ T lymphocytes

We isolated mononuclear cells from the spleen of HIV-1_{JR-CSF}-infected and mock-infected mice and then analyzed them by flow cytometry. As shown in Fig. 4A, the percentage of CD4⁺ T lymphocytes in the spleen of HIV-1_{JR-CSF} mice was smaller than that of mock-infected mice by 2.7-fold ($P=0.003$), showing that HIV-1_{JR-CSF}-infected mice had significantly fewer splenic CD4⁺ T lymphocytes. Moreover, the percentage of splenic CD4⁺CD45RA[−] memory T lymphocytes in HIV-1_{JR-CSF}-infected mice was smaller than that in the mock-infected mice ($P=0.007$), whereas the percentages of splenic CD4⁺CD45RA⁺ naïve T lymphocytes were indifferent ($P=0.17$) (Fig. 4B). In mock-infected mice, a significant fraction of CD4⁺CD45RA[−] T lymphocytes were CCR5⁺ memory T lymphocytes (Fig. 4C). In contrast, in HIV-1_{JR-CSF}-infected mice, we found approximately 20-fold reduction in the percentage (Fig. 4C) and 100-fold reduction in the number of CD4⁺CD45RA[−]CCR5⁺ memory T lymphocytes (data not shown). These results suggest that the CCR5-expressing memory CD4⁺ T lymphocytes are depleted by direct R5 HIV-1 infection and that such reduction of CCR5-expressing CD4⁺ T lymphocytes would lead to the decrease in whole memory CD4⁺ T lymphocytes.

Preferential HIV-1 productive infection in CD4-negative effector memory T lymphocytes

To characterize the immunophenotypes of HIV-1 productively infected cells in NOG-hCD34 mice, splenic mononuclear cells from

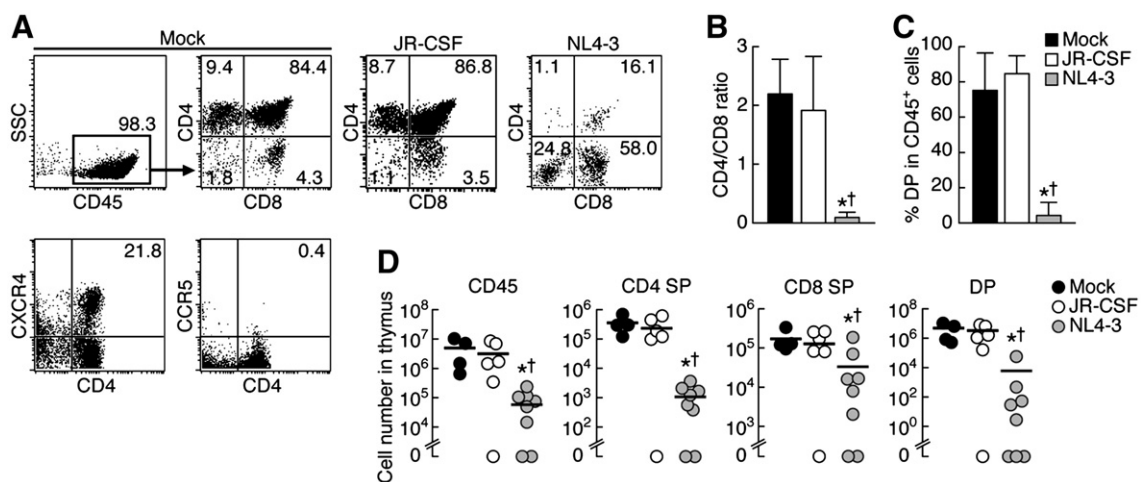


Fig. 2. Thymopathy in X4 HIV-1-infected mice. (A) Representative profile of flow cytometric analysis in thymi of mock-, HIV-1_{JR-CSF}- and HIV-1_{NL4-3}-infected mice. The numbers in dot plots indicate the percentage of cells in CD45⁺ thymocytes. (B and C) CD4/CD8 ratio (B) and the percentages of DP cells in CD45⁺ thymocytes (C) in mock-infected ($n=4$), HIV-1_{JR-CSF}-infected ($n=5$), and HIV-1_{NL4-3}-infected ($n=6$) mice. (D) Number of CD45⁺, CD4 SP, CD8 SP, and DP cells in thymi of mock-infected ($n=4$), HIV-1_{JR-CSF}-infected ($n=6$), and HIV-1_{NL4-3}-infected ($n=8$) mice. The horizontal bars in D show the average values, and the error bars in B and C show standard deviations. Asterisks indicate statistical significance ($P<0.05$) when compared to mock-infected mice, and daggers indicate statistical significance when compared to HIV-1_{JR-CSF}-infected mice.

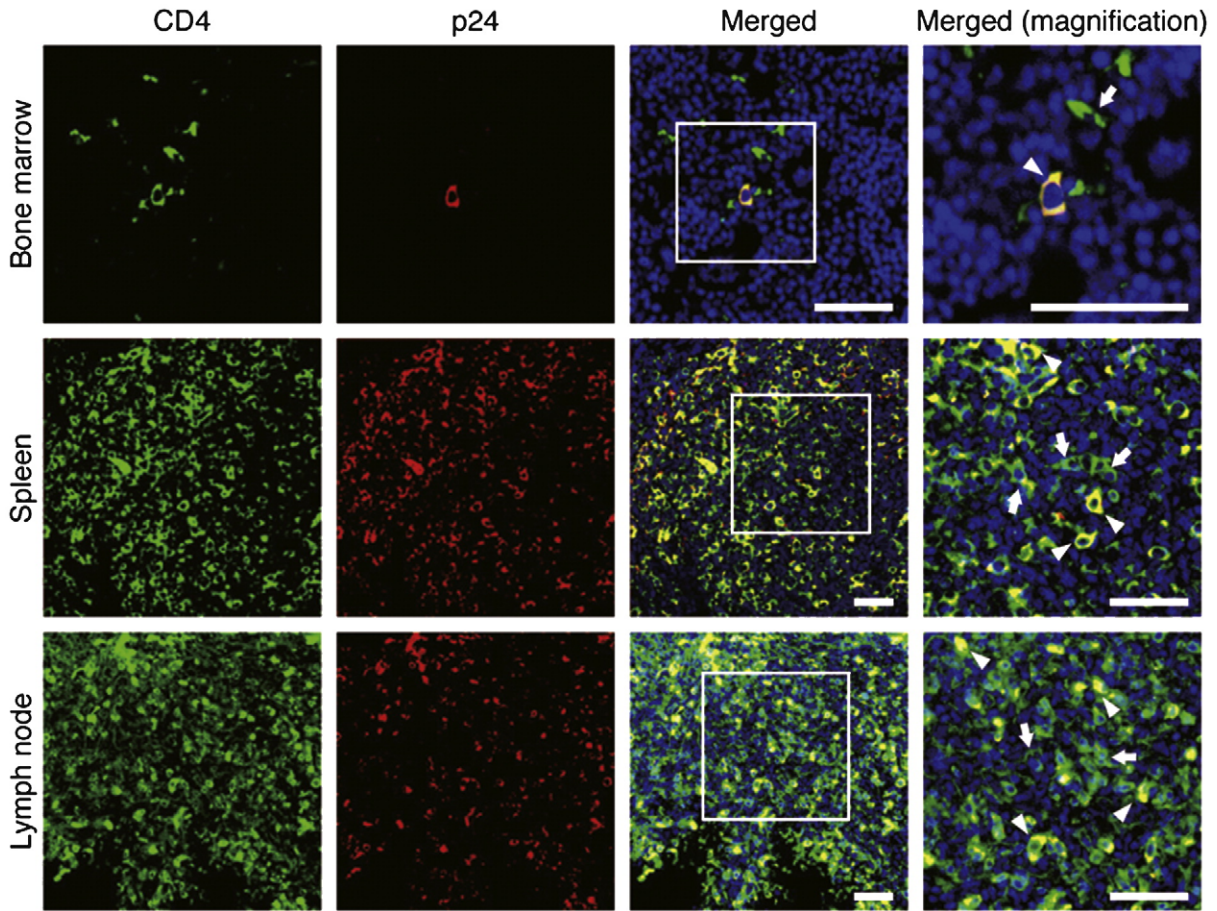


Fig. 3. Histological analysis on R5 HIV-1-infected mice. Representative immunohistological analysis of CD4 (green) and HIV-1 p24 (red) in the slices of bone marrow, spleen, and lymph nodes of HIV-1_{JR-CSF}-infected NOG-hCD34 mice. The low magnification images of the bone marrow slices were taken at $\times 80$, and the high magnification images were taken at $\times 160$. The low magnification images of the spleen and lymph nodes slices were taken at $\times 40$, and the high magnification images were taken at $\times 80$. The areas enclosed with the white squares were enlarged. The arrows point at representative CD4⁺ cells and the arrowheads point at representative CD4⁺p24⁺ cells. Scale bars, 50 μm .

HIV-1_{JR-CSF}-infected mice were further analyzed for HIV-1 antigen p24 and the expression of lymphocyte surface markers. The anti-p24 antibody that we used did not react with any of the cells isolated from the mock-infected mice (Fig. 5A), as reported previously (Okuma et al., 2008). A significant fraction of splenic leukocytes expressed HIV-1 p24 and thus was productively infected with HIV-1 (Fig. 5A). The productively infected cells expressed surface CD3 but lacked surface CD4 (Figs. 5B and C). On average, over 90% of the p24⁺ cells were CD3⁺, yet only about 5% of these cells expressed surface CD4 (Fig. 5C). Also, p24-expressing cells were positive for CD45RO but not for CD45RA, suggesting that they were memory T lymphocytes ($73.7 \pm 24.3\%$ for CD45RO⁺CD45RA⁻ in p24⁺ cells; Figs. 5D and E). Central memory T lymphocyte (T_{CM}) can be defined as a memory T lymphocyte that expresses CCR7, and effector memory T lymphocyte (T_{EM}) can be defined as a memory T lymphocyte that lacks CCR7 (Sallusto, Geginat, and Lanzavecchia, 2004). In p24-positive cells, $88.0 \pm 3.75\%$ was negative for CCR7 (Figs. 5D and F), suggesting that T_{EM} dominantly and productively infect with HIV-1.

Productive HIV-1 infection in activated and dividing lymphocytes

To investigate the activation status of the productively infected cells, splenic mononuclear cells were stained with anti-p24, anti-Ki67, and anti-CD69 antibodies. Ki67 antigen is exclusively expressed in proliferating cells, and CD69 is expressed on the surface of the activated cells at the early phase (Sereti et al., 2007; Vatakis et al., 2007). In splenic CD4⁺ T lymphocytes from mock-infected mice or p24-negative splenocytes from HIV-1_{JR-CSF}-infected mice, only a

minor fraction of the cells expressed either Ki67 or CD69 (Figs. 6A and B). In contrast, the majority of p24-positive splenocytes from HIV-1_{JR-CSF}-infected mice expressed Ki67 and/or CD69 (Figs. 6A and B). Also, the percentage of cells positive for both Ki67 and CD69 were higher in p24-positive cells than in p24-negative splenocytes from HIV-1_{JR-CSF}-infected mice and in splenic CD4⁺ T lymphocytes from mock-infected mice (Fig. 6B). These results indicate that a significantly higher frequency of p24-positive cells is activated and/or proliferating cells. Notably, although the frequency was significantly low, we could detect Ki67⁻CD69⁻ resting T lymphocytes in p24-positive cells (Figs. 6A and B).

To further analyze the cell cycle of HIV-1 productively infected cells (i.e., p24-positive cells), we carried out Hoechst staining, which quantifies DNA content of the cells. Ki67 staining in combination with the Hoechst staining will sort cells into those in G₀/G_{1a}, G_{1b}, and S/G₂/M phases of the cell cycle (Wilpshaar et al., 2000). As shown in Fig. 6C, non-stimulated human peripheral blood leukocytes (PBLs) predominantly exist in G₀/G_{1a} phases (Ki67⁻Hoechst^{low}, lower left in the quadrant), while PHA-activated human PBLs predominantly exist in cycling G_{1b} phase (Ki67⁺Hoechst^{low}, upper left in the quadrant) and S/G₂/M phases (Ki67⁺Hoechst^{high}, upper right in the quadrant). By using this method, we observed that p24-positive cells contained a significantly higher frequency of cells in the G_{1b} phase. In addition, the percentage of p24-positive cells in S/G₂/M phases was significantly higher than CD4⁺ splenocytes from mock-infected mice (Figs. 6D and E). These findings indicate that the majority of HIV-1-producing cells in the spleen of R5 HIV-1-infected mice are activated and in cycling phase. On the other hand, we detected the p24-

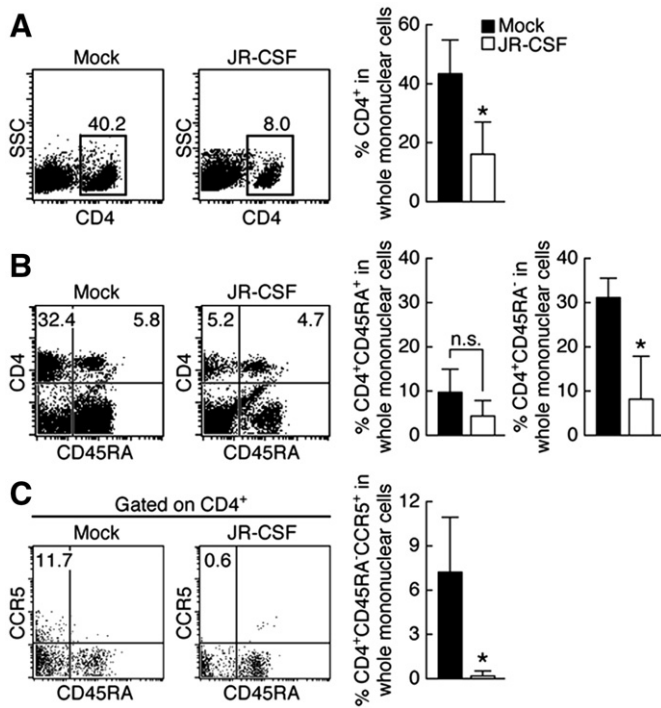


Fig. 4. The effect of R5 HIV-1 infection on the splenic CD4⁺ T lymphocyte population. (A–C) Staining of splenic nucleated cells from the spleen of mock-infected ($n = 4$) and HIV-1_{JR-CSF}-infected ($n = 4$) mice were stained with CD4 (A), CD4 and CD45RA (B), and CCR5, CD4, and CD45RA (C). Representative profiles are shown, and the numbers in dot plots indicate the percentage of cells in CD45⁺ splenic human leukocytes (A and B) or in CD4⁺ cells (C). The graphs show the percentages of cells possessing each phenotype in whole mononuclear cells. The error bars show standard deviations. Asterisks indicate statistical significance ($P < 0.05$) when compared to mock-infected mice.

positive splenocytes in G₀/G_{1a} phases, although the frequency was significantly lower than p24-negative splenocytes or CD4⁺ splenocytes from mock-infected mice (Figs. 6D and E). These data suggest that a fraction of resting cells productively infects HIV-1. Moreover, we detected the significantly higher percentage of cells in S/G₂/M phases in splenic p24-negative cells of HIV-1_{JR-CSF}-infected mice when comparing to that in splenic CD4⁺ T lymphocytes of mock-infected mice (Figs. 6D and E).

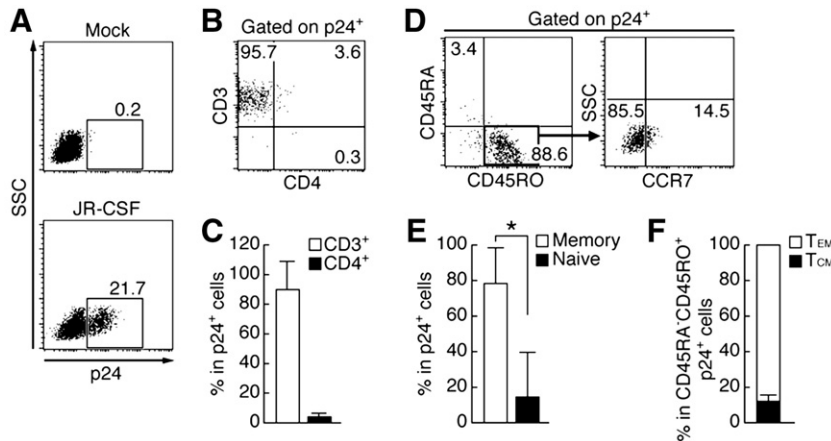


Fig. 5. Phenotype of productively infected p24⁺ cells in the spleen of R5 HIV-1-infected mice. (A) Representative profiles of flow cytometric p24 staining in splenic nucleated cells of mock-infected ($n = 4$) and HIV-1_{JR-CSF}-infected ($n = 6$) mice. The numbers indicate the percentage of cells in splenic nucleated cells. (B and C) Staining of splenic nucleated cells of HIV-1_{JR-CSF}-infected mice for p24, CD3, and CD4. Representative profiles are shown in B, and the numbers in each quadrant indicate the percentage of cells in p24⁺ cells. The percentages of each population in p24⁺ cells are shown in C. (D–F) Staining of splenic nucleated cells of HIV-1_{JR-CSF}-infected mice for p24, CD45RA, CD45RO, and CCR7. Representative profiles are shown in D, and the numbers in each quadrant indicate the percentage of cells in p24⁺ cells (left) or in p24⁺CD45RA⁻CD45RO⁺ cells (right). The percentages of memory (CD45RA⁻CD45RO⁺) and naïve (CD45RA⁺CD45RO⁻) phenotyped cells in p24⁺ cells are shown in E. The percentages of T_{EM} (CCR7⁻CD45RA⁻CD45RO⁺) and T_{CM} (CCR7⁺CD45RA⁻CD45RO⁺) in p24⁺ cells are shown in F. The error bars in C, E, and F show standard deviations. Asterisks indicate statistical significance ($P < 0.05$).

Discussion

To investigate the mechanisms of CD4⁺ T lymphocyte depletion by HIV-1 infection, we utilize human CD34⁺ cells-transplanted NOG mice (Ito et al., 2002) and demonstrate that human CD4⁺ T lymphocytes were differentially affected by X4 and R5 HIV-1 infection (Figs. 1–4). X4 virus induced immediate depletion of both naïve and memory CD4⁺ T lymphocytes in periphery, while R5 virus gradually depleted memory CD4⁺ T lymphocytes in the PB (Fig. 1) and spleen (Fig. 4). Our data suggest that distinctive pathogenesis of X4 and R5 viruses in NOG-hCD34 mice was caused by thymopathy (Fig. 2) and preferential infection of activated and dividing T_{EM} (Figs. 5 and 6), respectively. This is the first report addressing the mechanisms and dynamics of HIV-1-induced CD4⁺ T lymphocyte depletion *in vivo*.

As previously shown in X4 SHIV-infected macaques (Ho et al., 2005; Nishimura et al., 2004), we observed the drastic loss of both naïve and memory T lymphocytes by X4 HIV-1-infected NOG-hCD34 mice (Fig. 1). We also found that CD4⁺ thymocytes in NOG-hCD34 mice abundantly express CXCR4 (Fig. 2A) and that the CD4⁺ thymocytes including DP and CD4 SP were preferentially reduced in HIV-1_{NL4-3}-infected mice (Fig. 2). It has been reported that intrathymic infection by X4 HIV-1 can lead to severe T lymphocytopenia (Berkowitz et al., 1998; Schnittman et al., 1990; Ye, Kirschner, and Kourtis, 2004). Therefore, our results suggest that the primary mechanism for naïve and memory T lymphocyte depletion in X4 virus infection can be attributed to impaired thymopoiesis caused by intrathymic infection.

In contrast to X4 HIV-1 infection, the depletion of PB CD4⁺ T lymphocytes was more gradual and less intense in R5 HIV-1 infection and was confined to CD45RA⁻ memory CD4⁺ T lymphocytes (Fig. 1D). The selective depletion of memory CD4⁺ T lymphocytes by R5 infection was also found in the spleen (Fig. 4). On the other hand, thymopathy was not detected in HIV-1_{JR-CSF}-infected mice (Fig. 2). These findings suggest that the selective depletion of memory CD4⁺ T lymphocytes in PB and spleen of HIV-1_{JR-CSF}-infected mice caused through a different mechanism from HIV-1_{NL4-3}, and the mechanisms are further discussed below.

To investigate the mechanisms of memory CD4⁺ T lymphocyte depletion in R5 HIV-1 infection in-depth, a series of flow cytometric analyses was carried out. The majority of p24⁺ productively infected cells in the spleen were CD3⁺ T lymphocytes (Figs. 5B and C). However, these infected cells were negative for surface CD4 (Figs. 5B

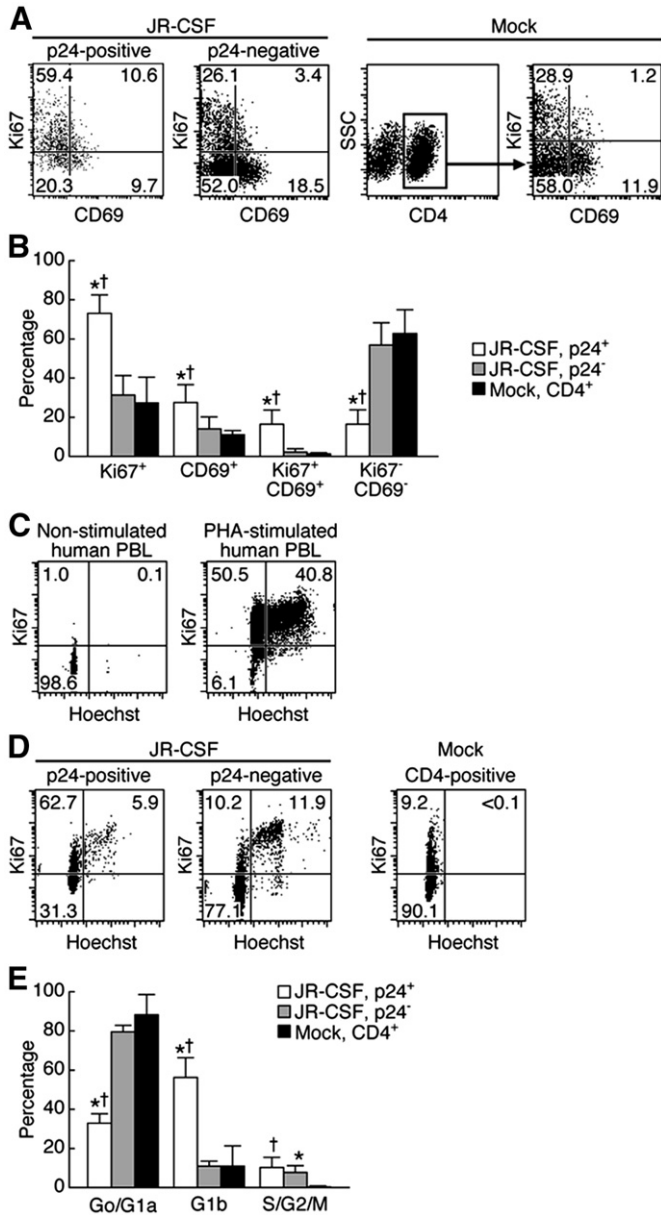


Fig. 6. Cell cycle analyses on productively infected p24⁺ cells in the spleen of R5 HIV-1-infected mice. (A and B) Staining of splenic nucleated cells of mock-infected (*n* = 3) and HIV-1_{JR-CSF}-infected (*n* = 4) mice for Ki67, CD69, and either CD4 or p24. Representative profiles are shown in A, and each number indicates the percentage of cells in each quadrant. The graph in B shows the average percentages of cells possessing each population. (C) A representative profile of cell cycle analysis on non-stimulated human PBL (left panel) and PHA-activated human PBL (right panel) by using anti-Ki67 antibody and Hoechst. Each number indicates the percentage of cells in each quadrant. Ki67[−] Hoechst^{low} (lower left in quadrant) indicates G₀/G_{1a} phase, while Ki67⁺ Hoechst^{low} (upper left in quadrant) and Ki67⁺ Hoechst^{high} (upper right in quadrant) indicate G_{1b} and S/G₂/M phases, respectively. (D and E) Staining of splenic nucleated cells of mock-infected mice (*n* = 4) for CD4, Ki67, and Hoechst, and HIV-1_{JR-CSF}-infected mice (*n* = 4) for p24, Ki67, and Hoechst. Representative profiles are shown in D, and each number indicates the percentage of cells in each quadrant. The graph in E shows the average percentages of cells in each population. The error bars in B and E show standard deviations. Asterisks indicate statistical significance (*P* < 0.05) when compared to the value of p24-negative cells in HIV-1_{JR-CSF}-infected mice, and daggers indicate statistical significance when compared to the value of CD4-positive cells in mock-infected mice.

and C), although immunohistological analysis revealed that splenic p24⁺ cells expressed CD4 molecules (Fig. 3). These results suggest that surface CD4 molecules are severely down-regulated following infection. In fact, it has been well documented that HIV-1 gene products such as *Nef* (Fackler, Alcover, and Schwartz, 2007; Roeth and

Collins, 2006), *Env* (Crise, Buonocore, and Rose, 1990), and *Vpu* (Bour and Strebel, 2003; Geleziunas, Bour, and Wainberg, 1994) have the potential to down-regulate CD4 molecules from the surface of infected cells (Lindwasser, Chaudhuri, and Bonifacio, 2007). Similar down-regulation of surface CD4 has also been reported in lymph nodes and PB of HIV-1-infected patients (Cheney et al., 2006; Kaiser et al., 2007; Marodon et al., 1999). Therefore, this down-regulation of surface CD4 molecules in HIV-1_{JR-CSF}-infected mice is physiologically relevant and can play a role in the reduction of CD4⁺ T lymphocytes.

In HIV-1_{JR-CSF}-infected mice, more than 80% of the productively infected cells were activated and in cycling phase (Fig. 6). It has been well known that activated cells massively produce HIV-1 virions (Ho et al., 1995). Therefore, this result suggests that the persistent viremia in R5 infection (Fig. 1A) is primarily due to the productive infection in the activated and proliferating cells. On the other hand, a fraction of infected cells were quiescent T lymphocytes negative for both activation and proliferation markers (Fig. 6). It is thought that HIV-1 cannot manifest productive infection in quiescent cells (Stevenson et al., 1990; Zack et al., 1990). However, studies on *ex vivo* infected human tonsil histocultures (Eckstein et al., 2001; Kinter et al., 2003), small intestines and cervix of SIV-infected rhesus macaques (Li et al., 2005; Zhang et al., 1999; Zhang et al., 2004), and HIV-1-infected patients (Zhang et al., 1999) have established that quiescent T lymphocytes residing in the lymphoid tissues are capable of supporting productive SIV or HIV-1 infection. Our results provide further support that productive infection of HIV-1 can take place in non-dividing cells, presumably resting T lymphocytes, in NOG-hCD34 mice. Productive infection not only in proliferative cells but also in quiescent cells may be an important factor in CD4⁺ T lymphocyte depletion and persistent virus infection.

The preferential infection of CD45RO⁺CD45RA[−] memory T lymphocytes with R5 HIV-1 is also the evidence supportive for the selective depletion of memory CD4⁺ T lymphocytes (Figs. 5D and E). Nevertheless, only 16.3 ± 9.7% of splenic CD4⁺ T lymphocytes expressed CCR5 in NOG-hCD34 mice, and the severe depletion of memory T lymphocytes in R5 HIV-1 infection cannot be explained by cell death caused by infection solely. In this regard, it has been reported that memory CD4⁺ T lymphocyte reduction in SIV-infected macaques can be initiated by specific disruption of T_{EM} due to its preferential infection in the acute phase (Centlivre et al., 2007; Mattapallil et al., 2005; Okoye et al., 2007). In response to the T_{EM} reduction, T_{CM} proliferates and supplies *de novo* T_{EM} (Sallusto, Geginat, and Lanzavecchia, 2004). However, Brenchley et al. (2004) and Okoye et al. (2007) have reported that R5 virus infection induces chronic immune activation in macaques, which leads to the attenuation of regenerative capacity of T_{CM} (Brenchley et al., 2004; Okoye et al., 2007). In addition to the depletion of T_{EM} by direct infection, the attenuation of regenerative potential of T_{CM} causes not only the loss of T_{CM} but also the shortage of T_{EM} and eventually leads to the reduction of whole memory T lymphocytes (Brenchley et al., 2004; Okoye et al., 2007). This hypothesis of the dynamics of CD4⁺ T lymphocyte depletion has been helpful for explaining the memory CD4⁺ T lymphocyte in effector sites of SIV-infected macaques. Our observations in HIV-1_{JR-CSF}-infected mice, the severe depletion of memory T lymphocytes despite the limited availability of CCR5-expressing CD4⁺ T lymphocytes and the preferential infection in T_{EM}, can be explained by the aforementioned hypothesis proposed in the previous literature (Brenchley et al., 2004; Okoye et al., 2007). Notably, we found that the frequency of cells in S/G₂/M phases elevated in splenic p24-negative cells of HIV-1_{JR-CSF}-infected mice when comparing to that in splenic CD4⁺ T lymphocytes of mock-infected mice (Figs. 6D and E). These data may explain that HIV-1 pathophysiology is caused by accelerated cells division, ultimately leading to the exhaustion of CD4⁺ T lymphocytes. Taken together, our findings suggest that the selective infection of T_{EM} may be an important event that governs CD4⁺ T lymphocyte depletion not

only in the effector sites of macaques during SIV infection but also in lymphoid organs during HIV-1 infection.

In summary, we showed differential CD4⁺ T lymphocyte reduction in R5 and X4 HIV-1 infection. We report for the first time the selective depletion of memory CD4⁺ T lymphocytes and the preferential infection of T_{EM} in an experimental model of R5 HIV-1 infection. Our data suggest that HIV-1 infection in T_{EM} can be an important step leading to CD4⁺ T lymphocyte decline. Our findings confirm the applicability of NOG-hCD34 mice as a useful model to study the dynamics of HIV-1 pathogenesis including CD4⁺ T lymphocytes depletion *in vivo*.

Materials and methods

Mice

NOD/SCID/IL-2R γ^{null} (NOG) mice (Ito et al., 2002) were obtained from the Central Institute for Experimental Animals (Kanagawa, Japan). The mice were maintained under specific pathogen-free conditions and were handled in accordance with the Regulation on Animal Experimentation at Kyoto University.

Purification and transplantation of cord blood-derived CD34 cells

The purification of cord blood-derived CD34 cells was conducted as described previously (Ishikawa et al., 2005; Ito et al., 2002). Fresh human cord blood was obtained with parent written informed consent from healthy full-term newborns and CD34 MicroBead Kit (Miltenyi Biotec Inc, Auburn, CA) was used to isolate hCD34⁺ cells according to the manufacturer's instructions. Cells were either stored at -80°C or immediately transplanted when newborn mice were available. CD34⁺ cells ($5\text{--}12 \times 10^4$) were intrahepatically injected into newborn mice of ages between 0 and 2 days after total radiation of 10 cGy per mouse in MBR-1520 x-ray irradiator (Hitachi Medico, Tokyo, Japan).

Peripheral blood collection and isolation of nucleated cells from organs

PB was routinely taken from NOG-hCD34 mice under ether anesthesia via retro-orbital venousplexus as described previously (Ishikawa et al., 2005). The red blood cells in the PB were lysed in preparation for flow cytometric analysis in $1 \times$ BD lysis buffer (BD Pharmingen, San Diego, CA). When the mice were sacrificed, PB was taken by cardiac puncture. Lymph nodes, thymi, spleen, and bone marrow were taken from HIV-1-infected and mock-infected mice upon sacrifice for histological or flow cytometric analysis. Lymph nodes and thymi were gently homogenized using a homogenizer pestle and spleens were crushed and rubbed on a steel mesh with 1-mm grids to generate single cell suspensions in RPMI 1640 supplemented with 4% fetal calf serum (FCS). To collect bone marrow, thigh bones were dissected at both ends and the interior was flushed with RPMI 1640 supplemented with 4% FCS. The cells were immediately used for flow cytometric analysis or stored in Cell Banker (Juji Field Inc., Tokyo, Japan) at -80°C until use. As there are some variations in the combination of antibodies used to study the human cell population in each mouse, the number of data collected for each surface marker may differ. Data used for any longitudinal analysis were taken from identical mice.

Flow cytometric analysis of human blood cells in transplanted mice

The staining for flow cytometric analysis was done with some modifications to the protocol previously described (Sato et al., 2008). Briefly, for the surface staining, the cells were blocked with FcR blocker (Miltenyi Biotec Inc) for 5 min at room temperature (RT) and then incubated with the appropriate antibodies at optimum

concentration in $1 \times$ phosphate-buffered saline (PBS) containing 2% FCS for 30 min at 4°C . Fluorescein isothiocyanate-conjugated (FITC-conjugated) anti-human CD19 (HD37; Dako, Tokyo, Japan), CD8 (DK25; Dako), CD14 (TUK4; Miltenyi Biotec Inc), CD4 (L3T4; eBioscience, San Diego, CA), CD3 (UCHT1; BD Pharmingen, San Diego, CA), CCR5 (3A9; BD Pharmingen), and CD303/BDCA2 (AC144; Miltenyi Biotec Inc) mouse IgG monoclonal antibodies (mAb); phycoerythrin-conjugated anti-human CD3 (UCHT1; Dako), CD4 (MT310; Dako), CD34 (AC136; Miltenyi Biotec Inc), CD11c (B-ly6; BD Pharmingen), CXCR4 (12G5; BD Pharmingen), CCR7 (FAB197; R&D systems, Abingdon, UK), and CCR5 (3A9; BD Pharmingen) mouse IgG mAb; biotinylated anti-human CD45 (H130; eBioscience), CD45RA (HI-100; BD Pharmingen), CD8 (RPA-T8; BD Pharmingen), CD4 (RPA-T4; BD Pharmingen), and mouse IgG mAb; peridinin-chlorophyll-conjugated (PerCP-conjugated) anti-human CD69 (L78; BD Immunocytometry Systems, San Jose, CA) mouse IgG mAb; PE-Cy5-conjugated anti-human HLA-DR (G46-6; BD Pharmingen) mouse IgG mAb; allophycocyanin-conjugated anti-human CD45RO (UCHL1; BD Pharmingen) and CD8 (DK25; Dako) mouse IgG mAb were used. Each antibody was controlled with appropriate isotype antibodies purchased from Dako and BD Pharmingen. Streptavidin-PerCP (SA-PerCP) was purchased from BD Immunocytometry Systems. Following the incubation, the cells were washed and further incubated with SA-PerCP for 30 min at 4°C , if needed. For the intracellular staining, the cells were permeabilized and fixed by treatment with BD Cytoperm/Cytofix solution (BD Pharmingen) and were stained with FITC-conjugated anti-HIV-1 p24 (clone 2C2) (Okuma et al., 2008) and anti-human Ki67 (B56; BD Pharmingen) mouse IgG mAb for 30 min at 4°C in $1 \times$ BD PermWash buffer (BD Pharmingen). For DNA staining to analyze cell cycle, the cells were incubated with Hoechst33342 (Invitrogen, Carlsbad, CA) for 30 min at 4°C as described previously (Wilpshaar et al., 2000). Data collection was performed on BD FACScan (BD Biosciences) for 3-color staining, BD FACSCalibur (BD Biosciences) for 4-color staining, and BD FACSCanto (BD Biosciences) for cell cycle analyses using Hoechst33342, and the obtained data were analyzed with CellQuest software (BD Immunocytometry System, San Jose, CA).

HIV-1 infection

NOG mice were injected intraperitoneally with RPMI 1640 ($n=8$) or 1×10^5 50% tissue culture infective doses (TCID₅₀) of HIV-1_{JR-CSF} ($n=7$) or HIV-1_{NL4-3} ($n=8$) between 12 and 13 weeks of ages. The viruses used were prepared by transfection as previously described (Sato et al., 2008). Infectious titers in the form of TCID₅₀ of each virus stock were determined by endpoint dilution with phytohemagglutinin-activated PBMCs as described (Koyanagi et al., 1997).

Detection of HIV-1 RNA in the plasma of infected mice

The detection of HIV-1 RNA in the plasma of the infected mice was routinely carried out using Amplicor HIV-1 monitor v1.5 according to the manufacturer's protocol (Roche Diagnostics, Mannheim, Germany).

Immunohistological analysis

Organs were fixed in $1 \times$ PBS containing 4% paraformaldehyde and embedded in OCT compound (Sakura Finetechnical, Tokyo, Japan) after immersion in 10%–20% gradient sucrose. The OCT embedded organs were then sliced and were permeabilized with 0.1% Triton-X at RT for 10 min, incubated three times with 10 mM glycine for 5 min and blocked with 5% normal goat serum at RT for 1 hr. The sections were then incubated with mouse anti-HIV-1 p24 (Kal-1; Dako) IgG mAb at 4°C overnight, followed by incubation with Alexa Fluor 488-conjugated goat anti-mouse IgG (Invitrogen) at RT for 2 hr. The sections were further incubated with biotinylated mouse anti-

human CD4 IgG mAb (RFT-4g; Southern Biotech, Birmingham, AL) at 4°C overnight, followed by incubation with Streptavidin–Alexa Fluor 647 (Invitrogen) and Hoeschst33342 at RT for 2 hr. All the antibody staining was performed in blocking solution. Images were acquired with a Leica TCS SP2 AOBS confocal laser microscope (Leica Microsystems, Heidelberg, Germany).

Statistical analysis

Data were expressed as an average with standard deviation. Significant differences between data groups were determined by Student's *t* test or paired *t* test. A *P* value less than 0.05 was considered significantly different.

Acknowledgments

We would like to thank Peter Gee (Institute for Virus Research, Kyoto University) for proofreading of our manuscript and Munetada Haruyama (the Department of Pediatrics, Kyoto University) for their generous help in our study. We also would like to express our appreciation for Ms. Kotubu Misawa's dedicated support. This work was supported by a Grant-in-Aid for Scientific Research on Priority Areas from the Ministry of Education, Culture, Sports, Sciences, and Technology of Japan; a Health and Labour Science Research Grant (Research on Publicly Essential Drugs and Medical Devices) from the Ministry of Health, Labor and Welfare of Japan; and Japan Human Science Foundation. K.S. was supported by Research Fellowships of the Japan Society for the Promotion of Science for Young Scientists. Y. K. was supported by a grant from the Naito Foundation.

Appendix A. Supplementary data

Supplementary data associated with this article can be found, in the online version, at doi:10.1016/j.virol.2009.08.011.

References

Ambrose, Z., KewalRamani, V.N., Bieniasz, P.D., Hatzioannou, T., 2007. HIV/AIDS: in search of an animal model. *Trends Biotechnol.* 25, 333–337.

Baenziger, S., Tussiwand, R., Schlaepfer, E., Mazzuchelli, L., Heikenwalder, M., Kurrer, M.O., Behnke, S., Frey, J., Oxenius, A., Joller, H., Aguzzi, A., Manz, M.G., Speck, R.F., 2006. Disseminated and sustained HIV infection in CD34⁺ cord blood cell-transplanted Rag2^{-/-}γc^{-/-} mice. *Proc. Natl. Acad. Sci. U. S. A.* 103, 15951–15956.

Berger, E.A., Murphy, P.M., Farber, J.M., 1999. Chemokine receptors as HIV-1 coreceptors: roles in viral entry, tropism, and disease. *Annu. Rev. Immunol.* 17, 657–700.

Berkowitz, R.D., Alexander, S., Bare, C., Linquist-Stepps, V., Bogan, M., Moreno, M.E., Gibson, L., Wieder, E.D., Kosek, J., Stoddart, C.A., McCune, J.M., 1998. CCR5- and CXCR4-utilizing strains of human immunodeficiency virus type 1 exhibit differential tropism and pathogenesis *in vivo*. *J. Virol.* 72, 10108–10117.

Bour, S., Strebel, K., 2003. The HIV-1 Vpu protein: a multifunctional enhancer of viral particle release. *Microbes. Infect.* 5, 1029–1039.

Brenchley, J.M., Price, D.A., Douek, D.C., 2006. HIV disease: fallout from a mucosal catastrophe? *Nat. Immunol.* 7, 235–239.

Brenchley, J.M., Schacker, T.W., Ruff, L.E., Price, D.A., Taylor, J.H., Beilman, G.J., Nguyen, P.L., Khoruts, A., Larson, M., Haase, A.T., Douek, D.C., 2004. CD4⁺ T cell depletion during all stages of HIV disease occurs predominantly in the gastrointestinal tract. *J. Exp. Med.* 200, 749–759.

Centlivre, M., Sala, M., Wain-Hobson, S., Berkhout, B., 2007. In HIV-1 pathogenesis the die is cast during primary infection. *AIDS* 21, 1–11.

Cheney, K.M., Kumar, R., Purins, A., Mundy, L., Ferguson, W., Shaw, D., Burrell, C.J., Li, P., 2006. HIV type 1 persistence in CD4⁻/CD8⁻ double negative T cells from patients on antiretroviral therapy. *AIDS Res. Hum. Retroviruses* 22, 66–75.

Crise, B., Buonocore, L., Rose, J.K., 1990. CD4 is retained in the endoplasmic reticulum by the human immunodeficiency virus type 1 glycoprotein precursor. *J. Virol.* 64, 5585–5593.

Ebert, L.M., McColl, S.R., 2001. Coregulation of CXC chemokine receptor and CD4 expression on T lymphocytes during allogeneic activation. *J. Immunol.* 166, 4870–4878.

Eckstein, D.A., Penn, M.L., Korin, Y.D., Scripture-Adams, D.D., Zack, J.A., Kreisberg, J.F., Roederer, M., Sherman, M.P., Chin, P.S., Goldsmith, M.A., 2001. HIV-1 actively replicates in naive CD4⁺ T cells residing within human lymphoid tissues. *Immunity* 15, 671–682.

Fackler, O.T., Alcover, A., Schwartz, O., 2007. Modulation of the immunological synapse: a key to HIV-1 pathogenesis? *Nat. Rev. Immunol.* 7, 310–317.

Geleziunas, R., Bour, S., Wainberg, M.A., 1994. Cell surface down-modulation of CD4 after infection by HIV-1. *FASEB J.* 8, 593–600.

Ho, D.D., Neumann, A.U., Perelson, A.S., Chen, W., Leonard, J.M., Markowitz, M., 1995. Rapid turnover of plasma virions and CD4 lymphocytes in HIV-1 infection. *Nature* 373, 123–126.

Ho, S.H., Shek, L., Gettie, A., Blanchard, J., Cheng-Mayer, C., 2005. V3 loop-determined coreceptor preference dictates the dynamics of CD4⁺-T-cell loss in simian–human immunodeficiency virus-infected macaques. *J. Virol.* 79, 12296–12303.

Ishikawa, F., Yasukawa, M., Lyons, B., Yoshida, S., Miyamoto, T., Yoshimoto, G., Watanabe, T., Akashi, K., Shultz, L.D., Harada, M., 2005. Development of functional human blood and immune systems in NOD/SCID/IL2 receptor γ chain^{null} mice. *Blood* 106, 1565–1573.

Ito, M., Hiramatsu, H., Kobayashi, K., Suzue, K., Kawahata, M., Hioki, K., Ueyama, Y., Koyanagi, Y., Sugamura, K., Tsuji, K., Heike, T., Nakahata, T., 2002. NOD/SCID/γc^{null} mouse: an excellent recipient mouse model for engraftment of human cells. *Blood* 100, 3175–3182.

Kaiser, P., Joos, B., Niederost, B., Weber, R., Gunthard, H.F., Fischer, M., 2007. Productive human immunodeficiency virus type 1 infection in peripheral blood predominantly takes place in CD4/CD8 double-negative T lymphocytes. *J. Virol.* 81, 9693–9706.

Kinter, A., Moorthy, A., Jackson, R., Fauci, A.S., 2003. Productive HIV infection of resting CD4⁺ T cells: role of lymphoid tissue microenvironment and effect of immunomodulating agents. *AIDS Res. Hum. Retroviruses* 19, 847–856.

Koyanagi, Y., Tanaka, Y., Ito, M., Yamamoto, N., 2008. Humanized mice for human retrovirus infection. *Curr. Top. Microbiol. Immunol.* 324, 133–148.

Koyanagi, Y., Tanaka, Y., Kira, J., Ito, M., Hioki, K., Misawa, N., Kawano, Y., Yamasaki, K., Tanaka, R., Suzuki, Y., Ueyama, Y., Terada, E., Tanaka, T., Miyasaka, M., Kobayashi, T., Kumazawa, Y., Yamamoto, N., 1997. Primary human immunodeficiency virus type 1 viremia and central nervous system invasion in a novel hu-PBL-immunodeficient mouse strain. *J. Virol.* 71, 2417–2424.

Li, Q., Duan, L., Estes, J.D., Ma, Z.M., Rourke, T., Wang, Y., Reilly, C., Carlis, J., Miller, C.J., Haase, A.T., 2005. Peak SIV replication in resting memory CD4⁺ T cells depletes gut lamina propria CD4⁺ T cells. *Nature* 434, 1148–1152.

Lindwasser, O.W., Chaudhuri, R., Bonifacino, J.S., 2007. Mechanisms of CD4 down-regulation by the Nef and Vpu proteins of primate immunodeficiency viruses. *Curr. Mol. Med.* 7, 171–184.

Lusso, P., 2006. HIV and the chemokine system: 10 years later. *EMBO J.* 25, 447–456.

Marodon, G., Warren, D., Filomio, M.C., Posnett, D.N., 1999. Productive infection of double-negative T cells with HIV *in vivo*. *Proc. Natl. Acad. Sci. U. S. A.* 96, 11958–11963.

Mattapallil, J.J., Douek, D.C., Hill, B., Nishimura, Y., Martin, M., Roederer, M., 2005. Massive infection and loss of memory CD4⁺ T cells in multiple tissues during acute SIV infection. *Nature* 434, 1093–1097.

McCune, J.M., 2001. The dynamics of CD4⁺ T-cell depletion in HIV disease. *Nature* 410, 974–979.

Moore, J.P., Kitchen, S.G., Pugach, P., Zack, J.A., 2004. The CCR5 and CXCR4 coreceptors – central to understanding the transmission and pathogenesis of human immunodeficiency virus type 1 infection. *AIDS Res. Hum. Retroviruses* 20, 111–126.

Nishimura, Y., Igarashi, T., Donau, O.K., Buckler-White, A., Buckler, C., Lafont, B.A., Goeken, R.M., Goldstein, S., Hirsch, V.M., Martin, M.A., 2004. Highly pathogenic SHIVs and SIVs target different CD4⁺ T cell subsets in rhesus monkeys, explaining their divergent clinical courses. *Proc. Natl. Acad. Sci. U. S. A.* 101, 12324–12329.

O'Brien, W.A., Hartigan, P.M., Martin, D., Esinhart, J., Hill, A., Benoit, S., Rubin, M., Simberloff, M.S., Hamilton, J.D., 1996. Changes in plasma HIV-1 RNA and CD4⁺ lymphocyte counts and the risk of progression to AIDS. Veterans Affairs Cooperative Study Group on AIDS. *N. Engl. J. Med.* 334, 426–431.

Okoye, A., Meier-Schellersheim, M., Brenchley, J.M., Hagen, S.I., Walker, J.M., Rohankhedkar, M., Lum, R., Edgar, J.B., Planer, S.L., Legasse, A., Sylwester, A.W., Piatak Jr., M., Lifson, J.D., Maino, V.C., Sodora, D.L., Douek, D.C., Axthelm, M.K., Grossman, Z., Picker, L.J., 2007. Progressive CD4⁺ central memory T cell decline results in CD4⁺ effector memory insufficiency and overt disease in chronic SIV infection. *J. Exp. Med.* 204, 2171–2185.

Okuma, K., Tanaka, R., Ogura, T., Ito, M., Kumakura, S., Yanaka, M., Nishizawa, M., Sugiura, W., Yamamoto, N., Tanaka, Y., 2008. Interleukin-4-transgenic hu-PBL-SCID mice: a model for the screening of antiviral drugs and immunotherapeutic agents against X4 HIV-1 viruses. *J. Infect. Dis.* 197, 134–141.

Pedroza-Martins, L., Gurney, K.B., Torbett, B.E., Uittenbogaart, C.H., 1998. Differential tropism and replication kinetics of human immunodeficiency virus type 1 isolates in thymocytes: coreceptor expression allows viral entry, but productive infection of distinct subsets is determined at the postentry level. *J. Virol.* 72, 9441–9452.

Roeth, J.F., Collins, K.L., 2006. Human immunodeficiency virus type 1 Nef: adapting to intracellular trafficking pathways. *Microbiol. Mol. Biol. Rev.* 70, 548–563.

Sallusto, F., Geginat, J., Lanzavecchia, A., 2004. Central memory and effector memory T cell subsets: function, generation, and maintenance. *Annu. Rev. Immunol.* 22, 745–763.

Sato, K., Aoki, J., Misawa, N., Daikoku, E., Sano, K., Tanaka, Y., Koyanagi, Y., 2008. Modulation of human immunodeficiency virus type 1 infectivity through incorporation of tetraspanin proteins. *J. Virol.* 82, 1021–1033.

Schnittman, S.M., Denning, S.M., Greenhouse, J.J., Justement, J.S., Baseler, M., Kurtzberg, J., Haynes, B.F., Fauci, A.S., 1990. Evidence for susceptibility of intrathymic T-cell precursors and their progeny carrying T-cell antigen receptor phenotypes TCRαβ⁺ and TCRγδ⁺ to human immunodeficiency virus infection: a mechanism for CD4⁺ (T4) lymphocyte depletion. *Proc. Natl. Acad. Sci. U. S. A.* 87, 7727–7731.

Sereti, I., Sklar, P., Ramchandani, M.S., Read, S.W., Aggarwal, V., Imamichi, H., Natarajan, V., Metcalf, J.A., Kovacs, J.A., Tavel, J., Davey, R.T., Dersimonian, R., Lane, H.C., 2007. CD4⁺ T cell responses to interleukin-2 administration in HIV-infected patients are

- directly related to the baseline level of immune activation. *J. Infect Dis.* 196, 677–683.
- Stevenson, M., Stanwick, T.L., Dempsey, M.P., Lamonica, C.A., 1990. HIV-1 replication is controlled at the level of T cell activation and proviral integration. *EMBO J.* 9, 1551–1560.
- Traggiai, E., Chicha, L., Mazzucchelli, L., Bronz, L., Piffaretti, J.C., Lanzavecchia, A., Manz, M.G., 2004. Development of a human adaptive immune system in cord blood cell-transplanted mice. *Science* 304, 104–107.
- Vatakis, D.N., Bristol, G., Wilkinson, T.A., Chow, S.A., Zack, J.A., 2007. Immediate activation fails to rescue efficient human immunodeficiency virus replication in quiescent CD4⁺ T cells. *J. Virol.* 81, 3574–3582.
- Wilpshaar, J., Falkenburg, J.H., Tong, X., Noort, W.A., Breese, R., Heilman, D., Kanhai, H., Orschell-Traycoff, C.M., Srouf, E.F., 2000. Similar repopulating capacity of mitotically active and resting umbilical cord blood CD34⁺ cells in NOD/SCID mice. *Blood* 96, 2100–2107.
- Ye, P., Kirschner, D.E., Kourtis, A.P., 2004. The thymus during HIV disease: role in pathogenesis and in immune recovery. *Curr. HIV Res.* 2, 177–183.
- Zack, J.A., Arrigo, S.J., Weitsman, S.R., Go, A.S., Haislip, A., Chen, I.S., 1990. HIV-1 entry into quiescent primary lymphocytes: molecular analysis reveals a labile, latent viral structure. *Cell* 61, 213–222.
- Zhang, Z., Schuler, T., Zupancic, M., Wietgreffe, S., Staskus, K.A., Reimann, K.A., Reinhart, T.A., Rogan, M., Cavert, W., Miller, C.J., Veazey, R.S., Notermans, D., Little, S., Danner, S.A., Richman, D.D., Havlir, D., Wong, J., Jordan, H.L., Schacker, T.W., Racz, P., Tenner-Racz, K., Letvin, N.L., Wolinsky, S., Haase, A.T., 1999. Sexual transmission and propagation of SIV and HIV in resting and activated CD4⁺ T cells. *Science* 286, 1353–1357.
- Zhang, Z.Q., Wietgreffe, S.W., Li, Q., Shore, M.D., Duan, L., Reilly, C., Lifson, J.D., Haase, A.T., 2004. Roles of substrate availability and infection of resting and activated CD4⁺ T cells in transmission and acute simian immunodeficiency virus infection. *Proc. Natl. Acad. Sci. U. S. A.* 101, 5640–5645.